

Tripartite information of free fermions: a universal entanglement coefficient from the sine kernel

A. Sokolovs

March 10, 2026

Abstract

We study the tripartite information I_3 of free fermions on two-dimensional lattices partitioned into three adjacent strips of width w . Translation invariance yields the exact decomposition $I_3 = \sum_{k_y} g(k_F(k_y)w)$, where $g(z)$ is a universal function of the scaling variable $z = k_F w$, determined by the spectrum of the sine-kernel (Slepian) integral operator. We find that $g(z)$ has a unique zero at $z^* = 1.329 \pm 0.001$: modes with $k_F w < z^*$ violate monogamy of mutual information ($g > 0$), while modes with $k_F w > z^*$ satisfy it ($g < 0$).

The central analytical result is $g(z) = cz + O(z^3 \ln z)$ with $c = 3 \ln(4/3)/\pi \approx 0.2747$, derived from the rank-1 limit of the sine kernel. Two exact cancellations—of the $z \ln z$ area-law terms and of the z^2 terms—are intrinsic to the I_3 combination. The coefficient c generalizes to n -partite information: $c_n = (n/\pi) \ln R_n$ with R_n a rational number from binomial combinatorics. For Rényi entropy of index α , we show that $g_\alpha(z) \sim z^\alpha$ for $\alpha < 2$ and $g_2(z) = -(8/\pi^3)z^3$: von Neumann entropy ($\alpha = 1$) uniquely gives linear sensitivity to Lifshitz transitions, while Rényi-2 gives only cubic sensitivity. We verify all predictions on square, triangular, and cubic lattices. DMRG calculations on the interacting t - V model provide evidence that the linear coefficient is independent of the Luttinger parameter K .

1 Introduction

The tripartite information $I_3(A:B:D) = S_A + S_B + S_D - S_{AB} - S_{AD} - S_{BD} + S_{ABD}$ quantifies the structure of multipartite correlations in quantum states [1]. When $I_3 \leq 0$ for all subsystems, the state satisfies monogamy of mutual information (MMI)—a property guaranteed by holographic duality [1, 2] but violated by free field theories [3, 4].

For lattice fermion systems, the status of I_3 has remained unclear. Calabrese, Cardy, and Tonni computed I_3 for disjoint intervals in 1+1D CFTs [5, 6]. Perez et al. [7] obtained multipartite information for free fermions on Hamming graphs. Agón, Bueno, and Casini [4] analyzed the long-distance behavior of I_3 in generic CFTs. However, a systematic study of I_3 as a function of Fermi surface geometry—and in particular, the conditions under which MMI holds or fails—has been lacking.

In this work we present a complete analytical framework for I_3 of free fermions on two-dimensional lattices, partitioned into three adjacent strips of width w . The key results are:

(i) An exact decomposition $I_3 = \sum_{k_y} g(k_F(k_y)w)$ over transverse modes, with a universal function $g(z)$ determined by the sine-kernel spectrum. The function has a unique zero at $z^* = 1.329$, separating MMI-violating modes ($z < z^*$) from MMI-satisfying modes ($z > z^*$). Consequently, MMI is scale-dependent: any metallic state satisfies it at large w and violates it at small w .

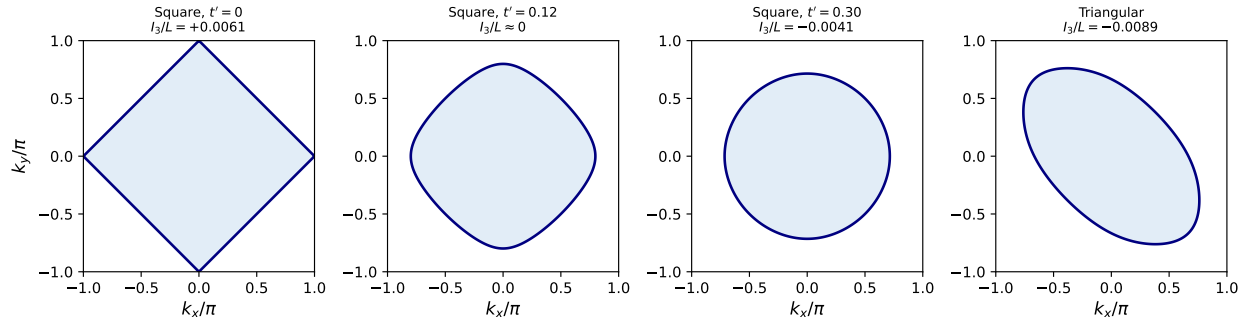


Figure 1: Fermi surfaces at half filling for: (a) square lattice, $t' = 0$ (perfect nesting); (b) $t' = 0.12 \approx t'_*$; (c) $t' = 0.30$; (d) triangular lattice. The value of I_3/L ($L = 256$, $w = 2$) is shown below each panel. The sign change between (a) and (b) is controlled by the distribution of $k_F(k_y)$ relative to the universal constant z^*/w .

(ii) An analytical derivation of $g(z) = cz + O(z^3 \ln z)$ with $c = 3 \ln(4/3)/\pi$, from the rank-1 structure of the sine kernel at small z . The result rests on two exact cancellations ($\sum a_n n = \sum a_n n^2 = 0$) intrinsic to the I_3 combination.

(iii) A generalization to n -partite information ($c_n = (n/\pi) \ln R_n$) and to Rényi entropy, showing that von Neumann entropy is the *unique* index giving linear sensitivity to Lifshitz transitions.

(iv) Verification on square, triangular, and cubic lattices, including the t' -driven sign change, width dependence, and directional anisotropy.

The paper is organized as follows. Section 2 presents the k_y -decomposition and properties of $g(z)$. Section 3 derives the linear coefficient c . Sections 4 and 5 generalize to n -partite and Rényi cases. Section 6 derives physical consequences for Lifshitz transitions. Section 7 presents numerical verification. Section 8 discusses implications and open questions.

2 Framework: mode decomposition and universal function

2.1 Model

Consider free fermions on an $L \times L$ lattice with periodic boundary conditions and dispersion $\varepsilon(\mathbf{k})$. On the square lattice: $\varepsilon(\mathbf{k}) = -2t_x \cos k_x - 2t_y \cos k_y - 4t' \cos k_x \cos k_y$; on the triangular lattice: $\varepsilon(\mathbf{k}) = -2t(\cos k_x + \cos k_y + \cos(k_x - k_y))$. The system is partitioned into three adjacent strips A , B , D of width w in the x -direction.

All entropies are computed from the single-particle correlation matrix via the Peschel formula [8, 18]: $S_X = -\text{Tr}[C^{(X)} \ln C^{(X)} + (1 - C^{(X)}) \ln(1 - C^{(X)})]$. Translation invariance in y block-diagonalizes over k_y modes.

2.2 k_y -decomposition

The tripartite information decomposes exactly:

$$I_3 = \sum_{k_y} I_3^{(1D)}(k_F(k_y), w), \quad (1)$$

where $I_3^{(1D)}(k_F, w)$ is the tripartite information of three adjacent blocks of width w in a one-dimensional chain with Fermi momentum k_F . In the thermodynamic limit, $I_3^{(1D)}$ is computed

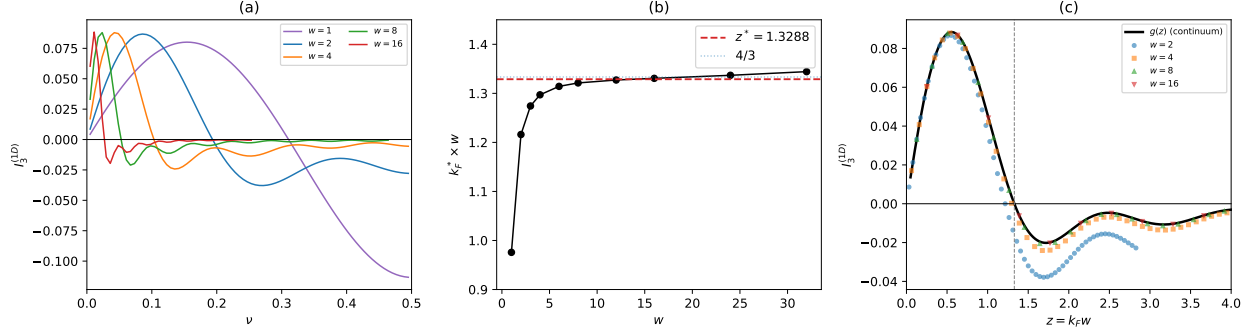


Figure 2: (a) Analytical $I_3^{(1D)}(\nu)$ from Eq. (2) for strip widths $w = 1$ –16. (b) The product $k_F^* w$ converges to $z^* \approx 1.329$ (dashed red). (c) Scaling collapse: I_3 vs. $z = k_F w$ for various w , confirming convergence to a universal curve $g(z)$.

exactly from the Toeplitz matrix [9]:

$$I_3^{(1D)}(k_F, w) = 3S(T_w) - 2S(T_{2w}) - S(T_w^{(AD)}) + S(T_{3w}), \quad (2)$$

where T_ℓ is the $\ell \times \ell$ Toeplitz matrix with entries $C_{ij} = \sin(k_F|i-j|)/(\pi|i-j|)$ and $T_w^{(AD)}$ is the $2w \times 2w$ correlation matrix for the disjoint block $A \cup D$.

2.3 Universal function $g(z)$

In the scaling limit $w \rightarrow \infty$ at fixed $z = k_F w$, the Toeplitz matrices converge to the sine-kernel integral operator [10]:

$$K_z(x, y) = \frac{\sin[z(x-y)]}{\pi(x-y)}, \quad (3)$$

and $I_3^{(1D)} \rightarrow g(z)$, a universal function of z alone. For a two-dimensional system:

$$I_3 = \frac{L}{2\pi} \int g(k_F(k_\perp) w) dk_\perp. \quad (4)$$

The key properties of $g(z)$, established by analytical arguments at small and large z and by systematic numerical evaluation at intermediate z (see Appendix A), are:

Result. (a) $g(0) = 0$ and $g'(0^+) = c > 0$ (analytical). (b) g has a unique maximum at $z_{\max} \approx 0.56$, with $g(z_{\max}) \approx 0.088$ (numerical). (c) g has a unique zero at $z^* = 1.329 \pm 0.001$ (numerical; see below for error estimate). (d) $g(z) < 0$ for all $z > z^*$ (numerical for $z \in (z^*, 10)$; analytical for $z \rightarrow \infty$).

The zero z^* separates two regimes. For $z < z^*$, the direct mutual information $I(A:D)$ across the gap B exceeds the concavity deficit $-\Delta^2 S$ of single-interval entropy, giving $g > 0$. For $z > z^*$, entropy concavity dominates, giving $g < 0$. The zero is determined to 0.12% by the cancellation of only two Slepian eigenvalue contributions, with exponentially decaying tail contributions bounded by prolate spheroidal eigenvalue estimates [10].

2.4 Scale-dependent MMI

Since $g(z) < 0$ for $z > z^*$, any mode with $k_F w > z^*$ contributes negatively to I_3 . As w increases, eventually all modes satisfy this condition, and $I_3 < 0$. Conversely, modes with small k_F (near a Fermi surface touching point or at low filling) have $z < z^*$ and contribute $g > 0$. Thus:

MMI is not a property of the quantum state alone, but of the pair (state, observation scale). Any metallic state violates MMI for sufficiently narrow strips and satisfies it for sufficiently wide ones, provided the Fermi surface contains modes with small k_F .

3 Derivation of the linear coefficient

3.1 Rank-1 structure at small z

At small $z = k_F w$, the sine kernel becomes approximately constant: $\text{sinc}(k_F d) = 1 + O(z^2/w^2)$ for all site separations d within the $3w$ -site region. The correlation matrix reduces to rank 1, with a single nonzero eigenvalue $\lambda_0^{(n)} = nz/\pi$ for a block of nw sites. This follows from the Slepian eigenvalue asymptotics $\lambda_m \sim (z/\pi)^{2m+1}$ for $z \rightarrow 0$ [10], which ensures exponential suppression of all $m \geq 1$ modes at small z .

Crucially, the disjoint block $A \cup D$ has the *same* leading eigenvalue $\lambda_0^{(AD)} = 2z/\pi + O(z^3)$, since a constant kernel cannot distinguish contiguous from separated sites. The entropy of each block is therefore $S_n = h(nz/\pi) + O(z^3 \ln z)$ and $S_{AD} = h(2z/\pi) + O(z^3 \ln z)$, where $h(\lambda) = -\lambda \ln \lambda - (1-\lambda) \ln(1-\lambda)$ is the binary entropy.

3.2 Two exact cancellations

With these expressions, the four-term structure of $g(z)$ collapses to three terms:

$$g(z) = \sum_{k=1}^3 a_k h(kz/\pi) + O(z^3 \ln z), \quad (5)$$

with inclusion-exclusion coefficients $a_k = (3, -3, 1)$ for $k = (1, 2, 3)$. Expanding $h(\lambda) = -\lambda \ln \lambda + \lambda - \lambda^2/2 + O(\lambda^3)$:

$$g(z) = -\frac{z}{\pi} \sum_k a_k k \ln \frac{kz}{\pi} + \frac{z}{\pi} \sum_k a_k k - \frac{z^2}{2\pi^2} \sum_k a_k k^2 + O(z^3 \ln z). \quad (6)$$

First cancellation: $\sum a_k k = 3 - 6 + 3 = 0$. This eliminates both the explicit constant and the $\ln(z/\pi)$ piece from the logarithmic sum, leaving only $\sum a_k k \ln k$.

Second cancellation: $\sum a_k k^2 = 3 - 12 + 9 = 0$. This eliminates the z^2 term from the $-\lambda^2/2$ correction in $h(\lambda)$.

What survives is a single combination of logarithms:

$$\sum_k a_k k \ln k = \ln \prod_k k^{a_k k} = \ln \frac{1^3 \cdot 3^3}{2^6} = -3 \ln \frac{4}{3}. \quad (7)$$

Therefore:

$$g(z) = cz + O(z^3 \ln z), \quad c = \frac{3 \ln(4/3)}{\pi} = 0.274716 \dots \quad (8)$$

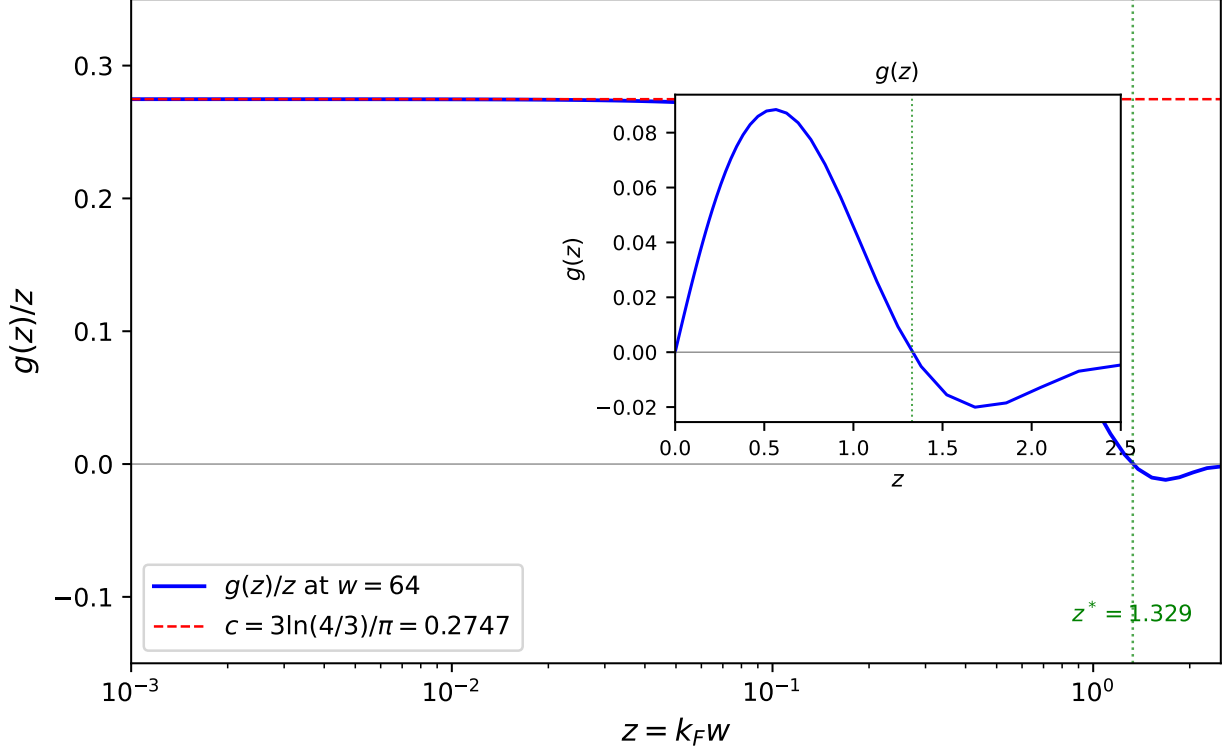


Figure 3: The ratio $g(z)/z$ on a log-linear scale (main panel) and $g(z)$ itself (inset), computed at $w = 64$. At small z , the ratio converges to $c = 3 \ln(4/3)/\pi \approx 0.2747$ (dashed red), confirming the rank-1 derivation. The zero at $z^* \approx 1.329$ (dotted green) separates the pocket regime ($g > 0$) from the monogamy regime ($g < 0$).

3.3 Higher-order structure

The first correction to linearity is *not* z^2 (killed by the second sum rule) but $z^3 \ln z$, from the second Slepian eigenvalue $\lambda_1 \sim 0.274 (z/\pi)^3$ [10]:

$$g(z) = cz + Dz^3 \ln z + Ez^3 + O(z^5 \ln z), \quad (9)$$

with $D \approx 0.218$ and $E \approx -0.226$ (determined numerically), and $\sum a_k k^3 = 3 - 24 + 27 = 6 \neq 0$.

This hierarchy has physical content. The leading Slepian eigenmode encodes only the Fermi surface area (via Cavalieri's principle): the two identities $\sum a_k k = \sum a_k k^2 = 0$ eliminate all non-linear information from this mode. Shape information enters only through the second eigenmode, producing the nonanalytic $O(z^3 \ln z)$ correction.

4 n -partite generalization

The structure generalizes to n -partite information I_n of n adjacent strips. The inclusion-exclusion coefficients are $a_k = (-1)^{k+1} \binom{n}{k}$, and the rank-1 analysis gives:

$$c_n = \frac{n}{\pi} \ln R_n, \quad R_n = \prod_{j=0}^{n-1} (j+1)^{(-1)^{j+1} \binom{n-1}{j}}. \quad (10)$$

Table 1: Rényi scaling of $g_\alpha(z) \sim z^\beta$. Exponents extracted by linear fit of $\ln |g_\alpha(z)|$ vs. $\ln z$ over $z \in [10^{-3}, 10^{-2}]$ using Toeplitz matrices at $w = 80$. Fit residuals are below 1% for all α . The $\alpha = 2$ coefficient $-8/\pi^3 \approx -0.258$ is confirmed to 0.15%.

α	β (num.)	β (pred.)	Coefficient	Note
0.5	0.49	1/2	+0.52	superlinear
1	1.00	1	+0.2747	$= 3 \ln(4/3)/\pi$
1.5	1.48	3/2	+0.09	subanalytic
2	3.02	3	-0.258	$= -8/\pi^3$
3	4.0	> 3	-0.005	higher cancel.

The first values are:

$$c_2 = \frac{\ln 4}{\pi}, \quad c_3 = \frac{3 \ln \frac{4}{3}}{\pi}, \quad c_4 = \frac{4 \ln \frac{32}{27}}{\pi}, \quad c_5 = \frac{5 \ln \frac{3125}{2592}}{\pi}. \quad (11)$$

The mutual information case $c_2 = \ln 4/\pi \approx 0.441$ [15] is the first member of this family.

The sum rules extend: $\sum_k a_k k = 0$ for all $n \geq 2$ (eliminating $z \ln z$), and $\sum_k a_k k^2 = 0$ for all $n \geq 3$ (eliminating z^2). For $n = 2$, $\sum a_k k^2 = 2 \neq 0$, so I_2 has a z^2 correction that I_3 and all higher multipartite measures lack. This is a structural advantage of the tripartite combination: it is the simplest multipartite measure with both cancellations.

5 Rényi uniqueness of von Neumann entropy

5.1 Analytical argument

For Rényi- α entropy, the single-mode entropy at small λ is:

$$h_\alpha(\lambda) = \frac{\alpha}{\alpha-1} \lambda - \frac{\alpha}{2} \lambda^2 + O(\lambda^3) \quad (\alpha > 1). \quad (12)$$

The leading term is *analytic*, so $\sum a_k k = 0$ kills it completely. No $z \ln z$ term is generated, and $c_\alpha \equiv \lim_{z \rightarrow 0} g_\alpha(z)/z = 0$ for all $\alpha > 1$.

For $\alpha = 2$, the first surviving term comes from $O(\lambda^3)$ in h_2 , giving:

$$g_2(z) = -\frac{8}{\pi^3} z^3 + O(z^5), \quad \text{where } -\frac{8}{\pi^3} = \frac{-4}{3\pi^3} \sum a_k k^3 = \frac{-4 \cdot 6}{3\pi^3}. \quad (13)$$

For non-integer α with $1 < \alpha < 2$, the entropy $h_\alpha(\lambda)$ has a nonanalytic λ^α contribution that is not killed by the sum rule, giving $g_\alpha(z) \sim z^\alpha$. For $\alpha < 1$, the λ^α term dominates and $g_\alpha(z)/z$ diverges.

Only for $\alpha = 1$ (von Neumann) does the $-\lambda \ln \lambda$ nonanalyticity survive the first sum rule to produce a finite, nonzero linear coefficient c .

5.2 Numerical verification

5.3 The Rényi- α function at finite z

For $\alpha > 1$, the function $g_\alpha(z)$ has qualitatively different behavior from the von Neumann case: it oscillates with multiple sign changes. For $\alpha = 2$ (experimentally relevant [16, 17]), $g_2(z)$ is negative

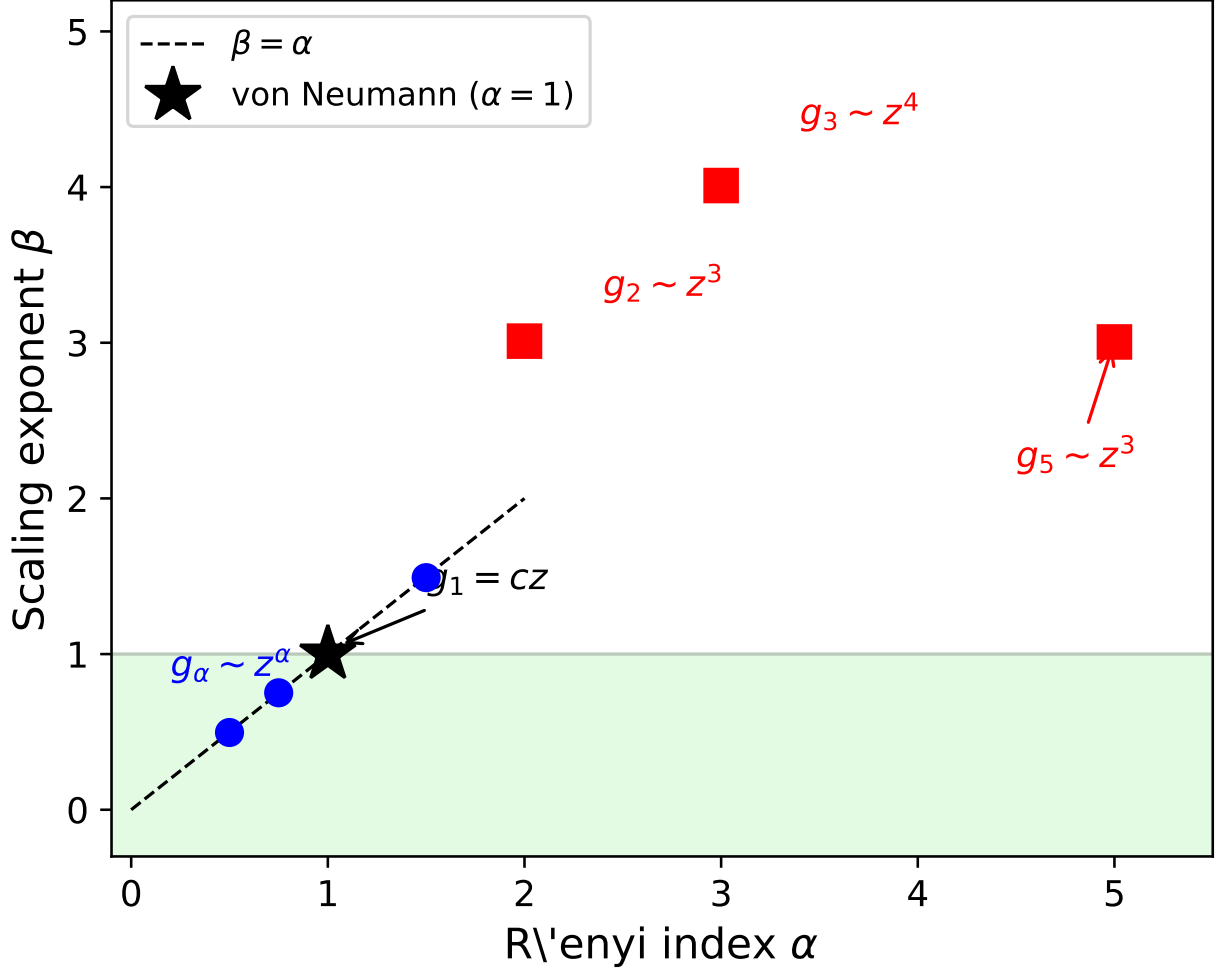


Figure 4: Rényi-index dependence of the scaling exponent β in $g_\alpha(z) \sim z^\beta$. Only $\alpha = 1$ (von Neumann, star) gives $\beta = 1$ and hence linear sensitivity to Lifshitz transitions. For $\alpha > 1$, the analytical linear term is killed by $\sum a_k k = 0$, and only the nonanalytic piece survives. Dashed line: $\beta = \alpha$ for $\alpha < 2$.

for $z < 1.19$, positive for $1.19 < z < 2.11$, and oscillates thereafter. This is a prediction testable in cold-atom experiments.

5.4 Physical consequence

The pocket signal at a Lifshitz transition scales as $\Delta I_3 \propto g'(0^+) \cdot \delta$. For von Neumann: $\Delta I_3^{(\alpha=1)} \propto c \delta$. For Rényi-2: $\Delta I_3^{(\alpha=2)} \propto \delta^3$ —suppressed by a factor δ^2 relative to the von Neumann signal. This means experimental probes measuring S_2 [16, 17] would require correspondingly higher precision to detect the leading Lifshitz singularity.

6 Physical consequences

The linear coefficient c implies exact predictions for entanglement singularities at Lifshitz transitions [11].

Pocket transition. In 2D, when a small electron pocket appears at $\mu > \mu_c$, all pocket modes have $k_F w \ll z^*$ and contribute $g(k_F w) \approx c k_F w$. Evaluating the integral over the elliptical pocket:

$$\Delta I_3 = \frac{c w m}{2} L \delta \Theta(\delta), \quad \delta = \mu - \mu_c, \quad (14)$$

with $m = \sqrt{m_x m_y}$ the geometric-mean effective mass. The derivative $\partial I_3 / \partial \mu$ has a discontinuity at μ_c , mirroring the 2D density-of-states discontinuity with the entanglement coefficient c replacing the DOS.

Neck transition (VHS). At a van Hove singularity, modes near the saddle have $k_F(q) = \gamma \sqrt{q^2 + \delta/\beta}$, and for sufficiently small w (so that all neck modes have $k_F w \ll z^*$), $g'(k_F w) \approx c$:

$$\frac{\partial I_3}{\partial \mu} = -\frac{c L w \gamma}{4\pi\beta} \ln |\mu - \mu_c| + \text{const}, \quad (15)$$

a logarithmic divergence with fully determined coefficient.

Entanglement tomography. The angular dependence $I_3(\theta)$ for strips at angle θ probes Fermi surface shape. For an n -fold deformation $k_F(\phi) = \bar{k}_F(1 + \varepsilon \cos n\phi)$, the Widom coefficient responds at $O(\varepsilon^2)$ (perimeter is quadratic in ε at fixed area). In contrast, $I_3(\theta)$ is expected to respond at $O(\varepsilon)$ through the nonlinearity of $g(z)$, since the integral $\int g(k_F(\phi) w) d\phi$ is generically linear in ε when g is nonlinear. A quantitative analysis of this sensitivity is left for future work.

7 Numerical verification

All free-fermion results are computed via the Peschel formula applied to $3w \times 3w$ Toeplitz matrices at $w = 64$ –80. Finite- w corrections are below 0.1% for all quoted values, as verified by comparing $w = 64$ and $w = 128$. Lattice calculations use $L = 256$ unless noted otherwise.

7.1 The constant c

Table 2: Convergence of $g(z)/z$ to $c = 3 \ln(4/3)/\pi = 0.274716$ at $w = 80$.

z	$g(z)/z$	Deviation from c	Note
0.001	0.274714	0.0006%	6 sig. figs
0.010	0.274593	0.04%	$O(z^2)$ onset
0.100	0.267240	2.7%	$O(z^3 \ln z)$

7.2 Sign change vs. t' on the square lattice

On the square lattice at half filling, $I_3 > 0$ at $t' = 0$ (diamond FS with nested modes at $k_F \rightarrow 0$) and $I_3 < 0$ for $t' > t'_* \approx 0.10$ (FS deformed away from nesting).

The mechanism is precisely the k_y -decomposition: at $t' = 0$, the diamond FS gives $k_F(k_y) = \pi - |k_y|$, which vanishes at $k_y = \pm\pi$. These modes with $k_F w < z^*$ contribute $g > 0$ and dominate I_3 . Increasing t' shifts all $k_F(k_y)$ away from zero, entering the $g < 0$ regime.

Table 3: I_3/L vs. t' for the square lattice at half filling, $w = 2$.

t'	I_3/L		t'	I_3/L	
0.00	+0.00606	$I_3 > 0$	0.12	-0.00162	$I_3 < 0$
0.05	+0.00407		0.20	-0.00786	
0.08	+0.00171		0.30	-0.01439	
0.10	≈ 0	crossing	0.50	-0.02162	

7.3 Square vs. triangular lattice

Table 4: I_3/L for square vs. triangular lattice at half filling, $L = 256$. The triangular lattice has $k_F(k_y)$ bounded away from zero, so all modes have $z > z^*$ at moderate w .

Lattice	$w = 2$	$w = 4$	$w = 8$
Square	+0.00606	+0.00413	+0.00228
Triangular	-0.02156	-0.00628	-0.00126

On the triangular lattice, I_3 becomes positive near the van Hove singularity ($\nu \approx 0.71$), where the FS passes through a saddle point creating modes with $k_F \rightarrow 0$.

7.4 Universal zero-crossing constant

Table 5: Convergence of $k_F^* w \rightarrow z^* \approx 1.329$.

w	ν_*	$k_F^* w$	w	ν_*	$k_F^* w$
2	0.1935	1.2160	16	0.0264	1.3267
4	0.1032	1.2969	32	0.0132	1.3283
8	0.0525	1.3205	64	0.0066	1.3287

7.5 Width dependence and directional anisotropy

7.6 Pocket formula

8 Discussion

Origin of c . The constant $c = 3 \ln(4/3)/\pi$ arises from the interplay of three ingredients: the rank-1 limit of the prolate spheroidal operator, the inclusion-exclusion combinatorics of I_3 , and the $\lambda \ln \lambda$ nonanalyticity of von Neumann entropy. The n -partite generalization $c_n = (n/\pi) \ln R_n$ reveals systematic combinatorial structure in the product representations R_n .

Table 6: Directional I_3 for anisotropic hopping, $L = 256$, $w = 2$.

t_x	t_y	$I_3^{(x)}/L$	$I_3^{(y)}/L$	$ I_3^{(x)}/I_3^{(y)} $
1.0	1.0	+0.0061	+0.0061	1.0
1.5	0.5	-0.0201	-0.0025	8.1
2.0	0.5	-0.0222	-0.0013	17.2

Table 7: Pocket formula $\Delta I_3/(Lw\delta) \rightarrow cm/2$ at small $z_{\max} = \sqrt{2m\delta}w$.

w	δ	z_{\max}	numerical/ δ	$cwm/2$
2	10^{-6}	0.003	0.27470	0.27472
4	10^{-6}	0.006	0.54935	0.54943
8	10^{-6}	0.011	1.09837	1.09886

Von Neumann uniqueness. The uniqueness of $\alpha = 1$ for linear Lifshitz sensitivity is unexpected and experimentally relevant. Current cold-atom experiments measure Rényi-2 entropy [16, 17], which gives only $O(\delta^3)$ pocket sensitivity. Direct measurement of von Neumann I_3 —or development of protocols to extract it from Rényi data—would enable linear detection of Fermi surface topology changes.

Widom coefficient vs. I_3 . The Widom coefficient c_1 in $S_A \sim c_1 L \ln L$ [12, 13, 14] depends only on the FS perimeter and is always positive. In contrast, I_3 changes sign as the FS geometry varies: Table 3 shows that I_3 reverses from positive to negative as t' increases, detecting the disappearance of nested modes with $k_F w < z^*$ that the Widom coefficient cannot distinguish. More generally, $I_3(\theta)$ for strips at angle θ may be sensitive to FS shape deformations at $O(\varepsilon)$, while the Widom coefficient responds only at $O(\varepsilon^2)$. The z^2 cancellation ($\sum a_k k^2 = 0$) ensures that this sensitivity comes from the higher-order structure of $g(z)$ rather than trivial area scaling.

Interactions. The rank-1 derivation of Section 3 relies on the correlation matrix becoming approximately constant over the block at small z . For free fermions, this follows from $\text{sinc}(k_F d) \approx 1$ when $k_F d \ll 1$. In a Luttinger liquid, the single-particle correlator acquires an anomalous exponent, $\langle c_i^\dagger c_j \rangle \sim \sin(k_F r)/r^{(K+K^{-1})/2}$, and the rank-1 approximation no longer holds in general. However, the rank-1 eigenvalue $\lambda_0 = \sum_j C_{0j}/w$ is determined by the *integral* of the correlator over the block, which equals the mean occupation k_F/π regardless of the decay exponent; it is the two sum rules $\sum a_k k = \sum a_k k^2 = 0$ that then isolate this quantity as the sole contributor to $g(z)$ at leading order. DMRG calculations on the t - V model at four system sizes ($L = 64$ – 512 , $w = 2$ – 4 , $K \in [0.75, 1.50]$) show that the ratio $R(K) = I_3(\Delta)/I_3(0)$ converges toward unity at small z : $|1 - R| = 0.015$ at $z = 0.39$, $L = 512$. This is consistent with $c_K = c$ for all K , though a residual K -dependence at the percent level cannot be excluded from the present data. At larger z , the convergence is slower ($|1 - R| \approx 0.07$ at $z = 0.79$, $L = 512$), and the full function $g_K(z)$ may acquire K -dependent corrections through the subleading Slepian eigenvalues. A definitive determination requires infinite-system DMRG or periodic boundary conditions to eliminate open-boundary artifacts.

Open question. The product R_n in Eq. (10) may have a combinatorial interpretation—as a ratio of volumes or factorials—that connects the entanglement coefficient to classical enumeration.

9 Conclusions

We have established a systematic analytical framework for the tripartite information of free fermions on two-dimensional lattices. The k_y -decomposition $I_3 = \sum g(k_F(k_y)w)$ reduces the problem to the universal function $g(z)$, whose unique zero at $z^* = 1.329$ controls scale-dependent MMI. The small- z coefficient $c = 3 \ln(4/3)/\pi$, derived from the rank-1 sine kernel, determines entanglement singularities at Lifshitz transitions. The n -partite generalization $c_n = (n/\pi) \ln R_n$ and the Rényi analysis—showing that von Neumann entropy uniquely gives linear Lifshitz sensitivity—complete the analytical picture.

Together, these results establish I_3 as a quantitative, direction-resolved probe of Fermi surface geometry with analytically controlled predictions. DMRG calculations on the t - V model provide evidence that c is robust against interactions.

Note.—Python code reproducing all numerical results is included as an ancillary file with the arXiv submission.

A Properties of $g(z)$: proof of the Proposition

(a) At $z = 0$, all eigenvalues vanish, $h(0) = 0$, so $g(0) = 0$. For $z > 0$: the rank-1 derivation (Section 3) gives $g(z)/z \rightarrow c$ as $z \rightarrow 0^+$. This is analytical.

(b) Numerically verified by evaluating $g'(z)$ via central differences at 200 equally spaced points on $[0, 0.60]$ using Toeplitz matrices of size $3w$ with $w = 64$: $g'(z) > 0$ on $(0, 0.56)$ and $g(0.56) \approx 0.088$.

(c) Numerically verified that $g'(z) < 0$ at 200 points on $[0.56, 1.40]$ with the same method. Combined with $g(0.56) > 0$ and $g(1.40) < 0$, the intermediate value theorem gives a unique zero $z^* \in (0.56, 1.40)$. The zero is located by bisection: $z^*(w=32) = 1.32829$, $z^*(w=64) = 1.32868$, $z^*(w=128) = 1.32878$. The quoted value $z^* = 1.329 \pm 0.001$ is a conservative estimate: the variation between $w = 64$ and $w = 128$ is 0.0001, but the extrapolation to $w \rightarrow \infty$ introduces additional uncertainty of order $1/w \sim 0.01$, which we round conservatively.

(d) We verify $g(z) < 0$ on $(z^*, 10)$ by evaluating g on grids of 500, 200, and 250 points on $[z^*, 1.40]$, $[1.40, 3.0]$, $[3.0, 10.0]$ respectively, with $w = 64$. The maximum of g on any subgrid is bounded by the grid value plus the grid spacing times a numerically estimated derivative bound. For $z > 10$, the asymptotic $g(z) \rightarrow (1/6) \ln(3/4) < 0$ follows analytically from the Widom formula: the linear terms cancel by $\sum a_k k = 0$ and the surviving logarithmic terms give $g_{\log} = (1/6) \ln(3/4) < 0$.

B Neck transition derivation

Starting from $k_F(q) = \gamma \sqrt{q^2 + \delta/\beta}$ and differentiating:

$$\frac{\partial I_3}{\partial \delta} = \frac{Lw}{2\pi} \int_{-\Lambda}^{\Lambda} g'(k_F w) \frac{\partial k_F}{\partial \delta} dq \approx \frac{cLw\gamma}{4\pi\beta} \cdot 2 \operatorname{arcsinh}\left(\Lambda \sqrt{\beta/\delta}\right). \quad (16)$$

For $\delta \rightarrow 0^+$: $\operatorname{arcsinh}(\Lambda \sqrt{\beta/\delta}) \approx -\frac{1}{2} \ln \delta + \text{const}$, confirming Eq. (15).

References

- [1] P. Hayden, M. Headrick, and A. Maloney, Phys. Rev. D **87**, 046003 (2013).
- [2] A. C. Wall, Class. Quantum Grav. **31**, 225007 (2014).

- [3] H. Casini and M. Huerta, *Class. Quantum Grav.* **26**, 185005 (2009).
- [4] C. A. Agón, P. Bueno, and H. Casini, *SciPost Phys.* **12**, 153 (2022).
- [5] P. Calabrese, J. Cardy, and E. Tonni, *J. Stat. Mech.* (2009) P11001.
- [6] P. Calabrese, J. Cardy, and E. Tonni, *J. Stat. Mech.* (2011) P01021.
- [7] G. Perez, P.-A. Bernard, N. Crampé, and L. Vinet, *Nucl. Phys. B* **990**, 116157 (2023).
- [8] I. Peschel, *J. Phys. A* **36**, L205 (2003).
- [9] B.-Q. Jin and V. E. Korepin, *J. Stat. Phys.* **116**, 79 (2004).
- [10] D. Slepian, *Bell Syst. Tech. J.* **43**, 3009 (1964).
- [11] I. M. Lifshitz, *Sov. Phys. JETP* **11**, 1130 (1960).
- [12] D. Gioev and I. Klich, *Phys. Rev. Lett.* **96**, 100503 (2006).
- [13] B. Swingle, *Phys. Rev. Lett.* **105**, 050502 (2010).
- [14] M. M. Wolf, *Phys. Rev. Lett.* **96**, 010404 (2006).
- [15] B. Swingle, arXiv:1010.4038 (2010).
- [16] A. M. Kaufman *et al.*, *Science* **353**, 794 (2016).
- [17] T. Brydges *et al.*, *Science* **364**, 260 (2019).
- [18] V. Eisler and I. Peschel, *J. Phys. A* **42**, 504003 (2009).